EUROfusion

WPJET1-CPR(18) 19604

E Peluso et al.

A New Tomographic Method for the Analysis of Bolometric Measurements on JET

Preprint of Paper to be submitted for publication in Proceeding of
30th Symposium on Fusion Technology (SOFT)

This work has been carried out within the framework of the EUROfusion Consortium and has received funding from the Euratom research and training programme 2014-2018 under grant agreement No 633053. The views and opinions expressed herein do not necessarily reflect those of the European Commission.

A New Tomographic Method for the Analysis of Bolometric Measurements on JET

E.Peluso[a*], T.Craciunescu[b], M.Gelfusa[a], A.Murari[c] , P.J.Carvalho[d], P.Gaudio[a] and JET Contributors[§]

EUROfusion Consortium, JET, Culham Science Centre, Abingdon, OX14 3DB, UK

[a]Department of Industrial Engineering, University of Rome "Tor Vergata", via del Politecnico 1, Roma, Italy

[b]National Institute for Laser, Plasma and Radiation Physics, Magurele-Bucharest, Romania

[c]Consorzio RFX (CNR, ENEA, INFN, Universita' di Padova, Acciaierie Venete SpA), Corso Stati

[d]Instituto de Plasmas e Fusão Nuclear, Instituto Superior Técnico, Lisbon, Portugal

The accurate quantification of the emitted radiation is an important element in the interpretation of Tokamak performance and in the design of experiments. The spatial distribution of the total emitted radiation is typically determined with quite sophisticated tomographic techniques. On JET, a new tomographic inversion method, based on the Maximum Likelihood, has been very recently developed for this purpose. Its main innovative aspect is the analytic estimate of the confidence intervals in the emitted radiation levels. The method is computationally quite fast and can therefore be applied on a routine basis. Together with a systematic use of phantoms, it can have several very interesting applications. In addition to allowing a specific optimisation of the tomography for the main plasma scenarios, it permits also a systematic evaluation of various instrumental issues such as the effect of the noise, the impact of missing channels and the influence of the geometry and of systematic errors in the reconstructions. These potentialities are shown with a systematic analysis of bolometric data collected on JET during the experiments with the ITER Like Wall.

Keywords: Tomography, Bolometry, Maximum Likelihood.

1. Introduction

In Tokamaks, the total emission of radiation is measured with specific detectors called bolometers. The bolometric diagnostic on JET is based on metal foil absorbers, which have a quite flat absorption in the wavelength regions of interest, the UV and SXR. These sensors integrate the radiation emitted along specific lines of sight (LOS, see Figure 1) and have operated for many years, providing good quality measurements. On the other hand, to determine the total radiated power, the measured line integrals have to be processed with suitable tomographic inversion algorithms. One of the main difficulties in interpreting traditional tomographic reconstructions resides in the fact that they do not naturally provide a confidence interval to be associated with their estimates. Therefore, particularly in the perspective of operation at high radiated fraction, a tomographic method capable of quantifying the uncertainties in the reconstructions on a routine basis would be very beneficial. Recently at JET a new method has been proposed[1], based on the Maximum Likelihood (ML), to evaluate the emissivity distribution including estimates of its uncertainties. Section 2 briefly summarises the mathematical background of the technique.

Any tomographic inversion is an ill-posed problem: more degrees of freedom with respect to measurements allow different solutions to exist at the same time. To complicate the task, every measurement is affected by noise and in normal operations also the possibility of untrustworthy or missing measurements has to be faced. In this paper, both the aforementioned issues have been considered to test the robustness of the ML methodology [2] on JET. As previously stated, Section 2 provides a brief description of the mathematical background of the ML; Section 3 reports the main results obtained testing systematically the methodology with *phantoms* to tackle the effect of the noise, considering also the systematic errors due to the electronics. Finally Section 4 has been dedicated to report the analysis regarding missing channels on the reconstruction in one of the most critical location of the main chamber.

2. Mathematical background

Bolometers are detectors looking at the plasma along different lines of sight and with different orientation (Fig.1). If the emissivity distribution is denoted by f and the measurements by g, the tomographic problem can be stated by the relation:

$$\overline{g_m} = \sum_{n=1}^{N_p} H_{mn}\overline{f_n}, \quad m = 1, \ldots, N_d \tag{1}$$

where:

- $\overline{g_m}$ is the mean measured data, over all zero mean noise realizations n_g:

$$g = \bar{g} + n_g \tag{2}$$

- $\overline{f_n}$ is the expected emissivity distribution corresponding to the mean data $\overline{g_m}$
- N_p is the total number of pixels, N_d is the total number of detectors

*Corresponding author: emmanuele.peluso@uniroma2.it

§ See the author list of "X. Litaudon et al 2017 Nucl. Fusion 57 102001

- H_{mn} represents the elements of the so called projection matrix and they account for the amount of emission from pixel n accumulated in the detector m. The calculation of the matrix H for bolometry is described in details in [1].

Assuming that the emission is a Poisson process and g_m is a sample from a Poisson distribution, whose expected value is g, then the probability of obtaining the measurement $g=\{g_m|m=1,\ldots,N_d\}$ if the image is $f=\{f_n|n=1,\ldots,N_p\}$ is given by the likelihood function:

$$L(g/f) = \prod_k \frac{1}{g_k!}(\bar{g})^{g_k} \times exp(\bar{g}) \quad (3)$$

The ML estimate is obtained by maximizing the above expression:

$$f_{ML} = argmax_f L(g/f) \quad (4)$$

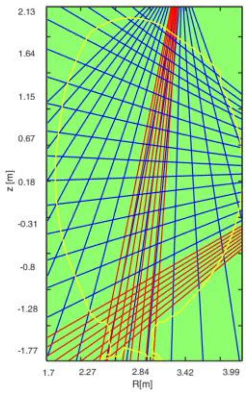

Figure 1 Schematic view of JET bolometric diagnostic layout.

For practical implementation an iterative solution for finding the ML estimate is the usual approach [3][4]:

$$f_n^{(k+1)} = \frac{f_n^{(k)}}{\sum_m H_{mn}} \sum_m \left(g_m / \sum_j H_{mj} f_j^{(k)}\right) H_{mn} \quad (5)$$

where k is indexing the iterations.

The ML method incorporates also a regularizing procedure that assumes smoothness on magnetic surfaces, obtained by solving the plasma equilibrium.

As relation (5) is working by means of multiplicative corrections, the following change of variable is a natural option:

$$y^{(k)} = ln\left[\hat{f}^{(k)}\right] \quad (6)$$

The measurements and the emissivity distribution are accompanied by a zero-mean noise, and therefore an expectation value can be defined as:

$$E\{y^{(k)}|f\} \stackrel{\text{def}}{=} ln\left(a^{(k)}\right) \quad (7)$$

and a deviation ε(k) from the expectation values:

$$y^{(k)} = ln\left(a^{(k)}\right) + \varepsilon^{(k)} \quad (8)$$

can also be defined.

Two approximations can be introduced in order to derive analytical expressions for retrieving ε(k) at each iteration. First, the noise can be considered small in comparison with the mean reconstruction:

$$\hat{f}^{(k)} = a^{(k)} exp\left(\varepsilon^{(k)}\right) \cong a^{(k)}\left[1 + \varepsilon^{(k)}\right] \quad (9)$$

It can be assumed also that the reconstruction algorithm is converging fast and therefore the projection of the current estimate is close to the noise free projection:

$$Ha^{(k)} \cong Hf \quad (10)$$

Introducing these approximations in (5) and separating the noise from the signal in the resulting expression, a couple of equations can be obtained (the reader is referred to [1] for a complete description):

$$f^{(k+1)} = f^k + diag\left[\hat{f}^{(k)}\right] diag\left[s^{-1}\right]$$
$$\left[H^T diag\left[H\hat{f}^{(k)}\right]^{-1} g - H^T I)\right] \quad (11)$$

$$\varepsilon^{(k+1)} = B^{(k)} n + \left[I - A^{(k)}\right]\varepsilon^{(k)} \quad (12)$$

where:

$$A^{(k)} = diag\left[\hat{f}^{(k)}\right] diag\left[s^{-1}\right] H^T diag\left[H\hat{f}^{(k)}\right]^{-1} H \quad (13)$$

$$B^{(k)} = diag\left[\hat{f}^{(k)}\right] diag\left[s^{-1}\right] H^T diag\left[H\hat{f}^{(k)}\right]^{-1} \quad (14)$$

Equation (11) allows retrieving the reconstruction from the noise free data while equation (12) allows the retrieval of the noise accompanying the current estimate. The latter can be re-written in the form:

$$\varepsilon^{(k)} = U^{(k)} n \quad (15)$$

where:

$$U^{(k+1)} = B^{(k)} + \left[I - A^{(k)}\right] U^{(k)} \quad (16)$$

is an operator applied to the noise in the original data. As the noise in the measured data n_g has a normal distribution, ε(k) is also characterized by a normal distribution, with the covariance:

$$K_\varepsilon^{(k)} = U^{(k)} K_{n_g} \left[U^{(k)}\right]^T \quad (16)$$

where K_{ng} is the covariance matrix for the data.

Therefore the covariance of the reconstructed image is derived from the covariance matrix for the measured data by means of the operator U.

3. Noise evaluation

Considering what has been stated in the previous sections, one major issue about tomography is the actual reliability of its reconstructions. Indeed a balance between an excellent match between measured and reconstructed projections and the realism of the results obtained has to be achieved; this is needed to avoid artefacts or unphysical effects in the reconstructions themselves. In addition to the just mentioned issues, the presence of random and/or systematic errors in the measurements sensibly increases the complexity and the reliability of the reconstructions themselves. For this reason a traditional approach [5] for the validation of tomographic codes requires the use of *phantoms*. In this section the effect of noise and of systematic uncertainties in the measurement is tackled. To achieve this goal, three phantoms have been considered with localized emissivities in different regions of the main chamber as Fig.2 shows. For each phantom, several noise realisations, obtained adding a normally distributed random noise, i.e $\mathcal{N}(0, \text{p})$ where $p \in [0.05, 0.1, 0.15, 0.2] \cdot \overrightarrow{prj}$, is added to the corresponding projections.

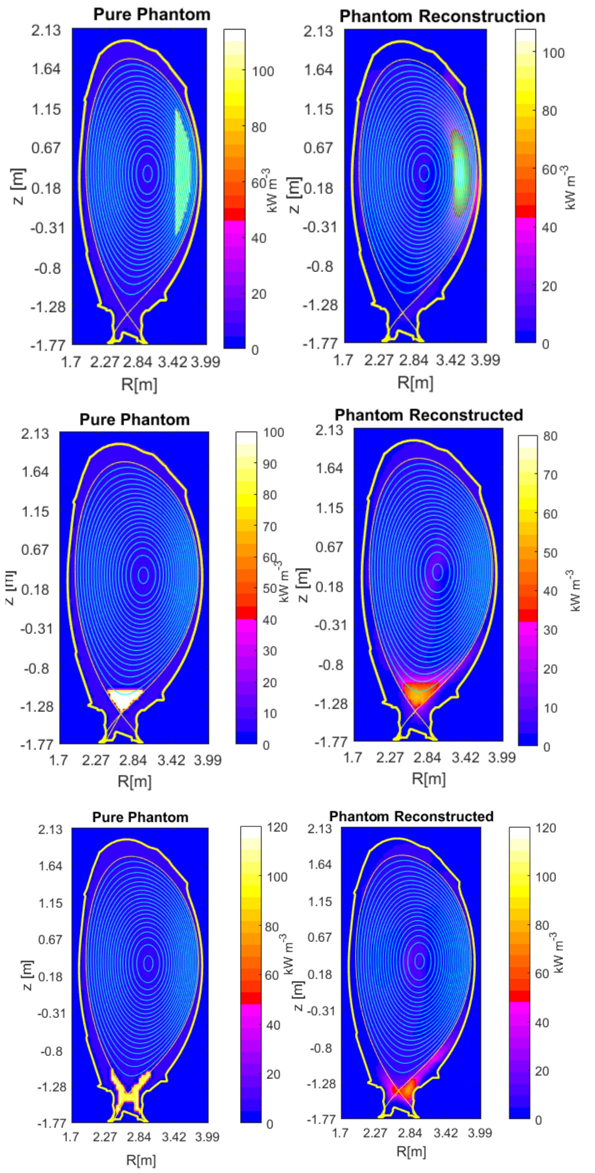

Figure 2 Three phantoms and reconstructions, standing for three typologies of emissions considered. From top to bottom: radiation from the core (“Core”), from the last closed surface(“LCFS”) and from the divertor (“Divertor”) region.

Table 1 Comparison between the uncertainties due to the noise on the bolometric measurements of the three phantoms in Fig2. and the actual noise added. The first column reports the noise added in percentage to the line integrals of the phantoms. The other columns show two values, again in percentage. The left one is the uncertainty without assuming any systematic error and the right one the uncertainty considering also the systematic error on the measurements

p%\Phantom	Core	LCFS	Divertor
5.0	[5.2,5.4]	[4.0,4.2]	[3.7,3.9]
10.0	[11.6,11.9]	[8.5,8.8]	[7.5,7.7]
15.0	[16.5,17.0]	[12.2,12.5]	[12.2,12.4]
20.0	[24.8,25.5]	[16.1,16.6]	[16.2,16.8]

After the reconstructions have been obtained applying the ML algorithm and both the averaged total radiated power and their averaged uncertainties have been computed.

The results have been reported in Table 1 where the systematic error due to the electronics of the acquisition system has been also considered for the uncertainty evaluation.

As it can be concluded from both Fig.2 and Table 1, the method is fully capable of reproducing the emissivities in different plasma regions and to evaluate the proper level of noise on the measurements. Furthermore, the averaged values of the uncertainty of the total radiation also increases, as expected and reported in Table 1, once the systematic error is propagated during the evaluation phase of the global uncertainty characteristic of each projection.

4. Effect of missing chords

During the DT campaign, due to high neutron fluxes certain detectors could be damaged with possible consequences on the quality of the reconstructions. To address the entity of this problem the following methodology has been adopted.

Measurements from the considered damaged detectors have been replaced by the average of the closest neighbours. The study here reported is based on an example borrowed from the pulse 92398 at 7.5s shown in Fig.3.

As it can be observed in Fig.3A the reconstruction shows a region of quite strong emissivity on the high field side corner, between divertor tiles 0 and 1, which is seen both by the vertical and by the horizontal arrays of bolometers.

For the reader’s convenience this feature has been also highlighted by the zoomed pictures at the bottom line of Fig 3.

To observe the behaviour of the reconstructions with missing channels, starting from the initial state (Fig.3A), two vertical LOS have been “removed” and their values averaged over their closest neighbours The obtained reconstruction can be observed in Fig.3B and shows that the tomographic reconstruction still provides a reasonable reconstruction of the original feature, even if slightly weaker.

A second step has consisted of removing two more horizontal LOS. Fig 3C reports the behaviour of the obtained reconstruction without the four measurements, which have been substituted with the averages of the closest channels. Again the emissivity in the corner is reconstructed acceptably.

On the other hand, removing even more LOS results in an unacceptable intensity of the feature.

A similar analysis has been performed also for other regions of the plasma cross section not so densely covered by LOS, like the low field side (LFS) region in Fig.3 where an extended zone with a high emissivity can be observed.

Fig.4 shows the effect of the failure of just one detector covering the considered area. Indeed the replacement of the measurement has a visible impact in the distribution of the emissivity that changes in the upper LFS region.

5. Conclusions

In this contribution several interesting aspects related to the bolometric tomographic inversion issue have been tackled using the ML method that has been

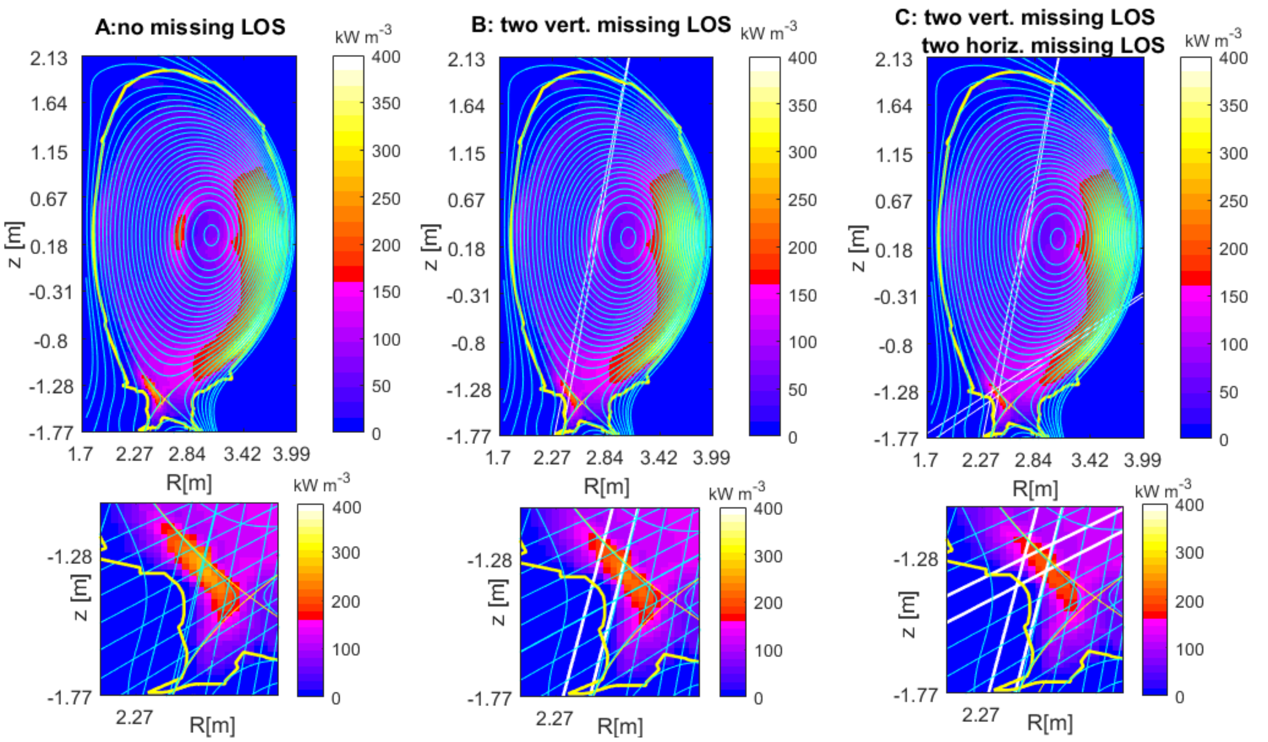

Figure 3 Top line: tomographic reconstructions using the ML methodology. From left to right: A: no missing LOS; B: two vertical LOS, plotted in white, have been averaged using the nearest projections; C: two vertical and two horizontal LOS in white have been considered as missing and their values averaged with the nearest ones. Bottom line: zoomed regions reproducing the studied feature. Again the replaced LOS have been reported in white.

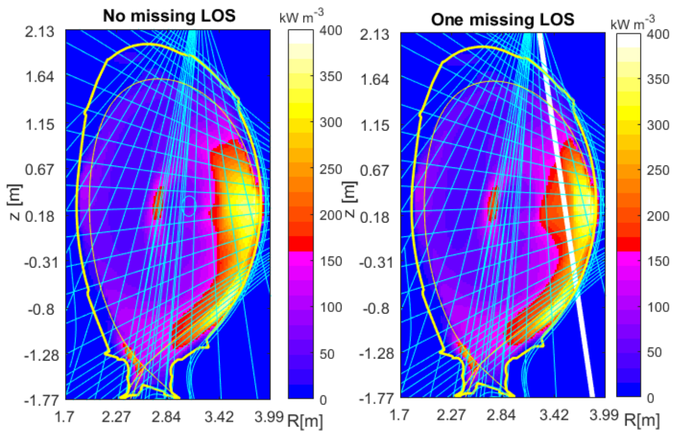

Figure 4 Left: Tomographic reconstruction obtained using all the available LOS; right: tomographic reconstruction without a vertical LOS (in white) in the low field side region less densely covered.

very recently developed [1]. First of all, considering Table 1, it can be stated that the ML method can provide reliable evaluations of the uncertainties of the reconstructed emissivity distributions in every region of the main chamber.

These estimates take into account both the known systematic effects due to the hardware, and the statistical uncertainties characterising the measured data.

Among the main relevant physical aspects that can benefit from the high degree of confidence on the uncertainties of the reconstruction and consequently on the derived physical quantities like the total radiated power, the power balance [6] is one of the most relevant. An accurate estimate of the error bars on the aforementioned quantity could be specifically useful when applied to the evaluation of the radiation fraction [7].

The second main topic considered in this contribution is the effect of missing LOS. The preliminary studies performed with the ML method, have revealed a good resilience of the bolometric reconstructions in the zones covered by sufficient lines of sight.

Acknowledgments

This work has been carried out within the framework of the EUROfusion Consortium and has received funding from the Euratom research and training programme 2014-2018 under grant agreement No 633053. The views and opinions expressed herein do not necessarily reflect those of the European Commission..

References

[1] T. Craciunescu et al., Rev. Sci. Instrum.89, (2018) 053504, doi

[2] Roy L .Strei, "Poisson Point Process", Springer, (2010) London, ISBN 978-1-4419-6922-4, doi

[3] H.H.Barrett et al, Phys. Med. Biol. 39, 833-346 1994.

[4] W. Wang et al. Phys. Med.Biol. 42, 2215–32 1997.

[5] L. C. Ingesson et al, Fusion Science and Technology, Volume 53, 2008 - Issue 2:doi

[6] J. Wesson, Tokamaks, 4th Edn., Oxford University Press, 2011, ISBN: 9780199592234

[7] A.Murari et al, Nucl.Fusion Vol.57, num.12 (2017), doi